Supplementary Information for

A dynamical motif comprising the interactions between antigens and CD8 T cells may underlie the outcomes of viral infections

Subhasish Baral, Rustom Antia, Narendra M. Dixit

Narendra M. Dixit
E-mail: narendra@iisc.ac.in

This PDF file includes:

Text S1. Predictions using an alternative model of CD8 T cell exhaustion. We examined the implications of CD8 T cell exhaustion triggered by cumulative rather than instantaneous antigenic stimulation. Following a previous formalism (1), we wrote:

$$\begin{aligned}\frac{dI}{dt} &= k_1 I\left(1-\frac{I}{I_{max}}\right) - k_2 IE \\ \frac{dE}{dt} &= k_3 \frac{IE}{k_p + I} - k_4 \frac{QE}{k_e + Q} \\ \frac{dQ}{dt} &= q_S\left(\frac{I}{\phi + I} - Q\right)\end{aligned} \quad [S1]$$

Here, Q represents the cumulative stimulation level, which increases with antigen load in a saturable manner with half-maximal constant ϕ and decays with the rate constant q_S. Q then determines the level of exhaustion, as opposed to the antigen load in Eq. 1 in the main text, and suppresses the effector response. The resulting motif is illustrated in Fig. S1A. Solving the equations above yielded clearance with low viral inoculum sizes and/or high initial effector pool size, immunopathology with intermediate sizes, and persistence with high viral inoculum sizes and/or low initial effector pool sizes (Fig. S1). The specific forms used to define exhaustion thus did not alter our key conclusions.

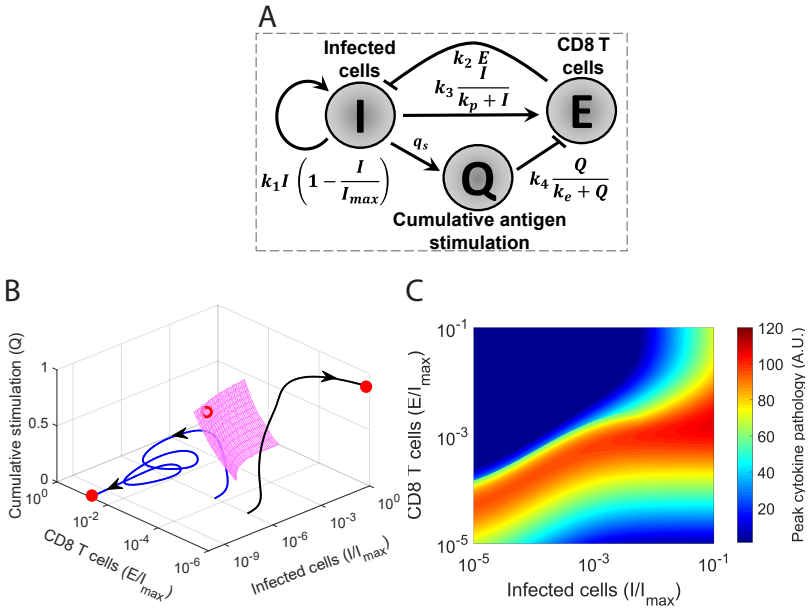

Fig. S1: Dynamical motif with exhaustion induced by cumulative antigen stimulation. (A) A schematic of the motif described in Text S1. (B) Phase diagram showing the stable steady states of persistence and clearance (filled red dots) separated by the basin boundary, shown in part (pink surface), on which the unstable steady state (open red dot) lies. Blue and black lines show representative trajectories leading to the two outcomes. Note that infection commences on the $Q = 0$ plane. (C) Cytokine pathology associated with a range of initial conditions illustrating maximum pathology near the basin boundary on the $Q = 0$ plane. Parameter values employed are as follows: $k_e = 0.8$; $q_s = 0.08$/day; and $\phi = 1000$ cells (1). The other parameters are the same as in Fig. 1.

Text S2. Linear stability analysis and robustness to parameter variations. The system in Eq. 1 in the main text with the exhaustion term away from saturation has 3 steady states. To determine the stability of these steady states, we performed linear stabililty analysis. The Jacobian matrix of the system is

$$\mathrm{A} = \begin{bmatrix} k_1 - \frac{2k_1 I}{I_{max}} - k_2 E & -k_2 I \\ \frac{k_3 k_p E}{(I+k_p)^2} - k_4 E & \frac{k_3 I}{I+k_p} - k_4 I \end{bmatrix} \quad [S2]$$

For the steady state representing clearance ($I = 0$ and $E \geq 0$), the Jacobian becomes

$$\mathrm{A} = \begin{bmatrix} k_1 - k_2 E & 0 \\ \frac{k_3 E}{k_p} - k_4 E & 0 \end{bmatrix} \quad [S3]$$

Thus, $trace(A) = k_1 - k_2 E$ and $det(A) = 0$, which would yield a line of stable fixed points as long as $E \geq \frac{k_1}{k_2}$.

For the steady state representing persistence ($I = I_{max}$ and $E = 0$), the Jacobian becomes

$$\mathrm{A} = \begin{bmatrix} -k_1 & -k_2 I_{max} \\ 0 & \frac{k_3 I_{max}}{I_{max}+k_p} - k_4 I_{max} \end{bmatrix} \quad [S4]$$

which has both eigenvalues real and negative if $\frac{k_3}{k_4} - k_p < I_{max}$. This steady state is thus stable as long as the latter inequality holds.

For the third steady state ($I = \frac{k_3}{k_4} - k_p$ and $E = \frac{k_1}{k_2}(1 - \frac{1}{I_{max}}(\frac{k_3}{k_4} - k_p))$), we can show that the signs of the elements of the Jacobian are

$$\mathrm{A} = \begin{bmatrix} + & - \\ - & 0 \end{bmatrix} \qquad [S5]$$

Thus, $det(A) < 0$, so that the eigenvalues have opposite signs. The steady state is therefore a saddle point.

The above behavior, with two stable steady states separated by a saddle point, is seen over wide ranges of parameter values (Fig. S2), suggesting that the key model predictions of the different outcomes of infection observed are robust to parameter choices. Indeed, parameter values exist where this bistability is lost and a single steady state is admitted. For instance, when k_3, the rate constant defining the mounting of the CD8 T cell response, is large, the only admitted stable steady state is viral clearance. When k_3 is zero, marking the absence of a CD8 T cell response, persistence becomes the sole stable steady state. The dependence on other parameters is similarly understood.

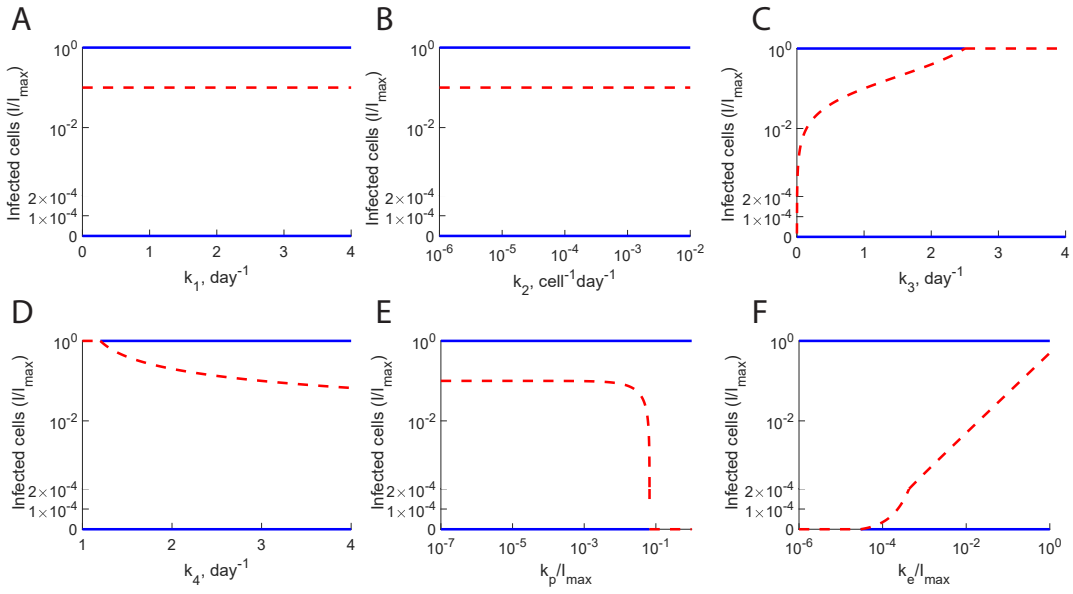

Fig. S2. Robustness of model predictions to parameter variations. The steady states of the model [Eq. 1] as each of the model parameters is varied are shown. Each panel presents results for one parameter variation. In each panel the upper and lower blue lines represent the stable steady states of persistence and clearance, respectively, and the red dashed line the unstable saddle point.

Text S3: Mathematical model of the motif with NK cells. The following equations describe the behavior of the motif with NK cells (Fig. 3):

$$\begin{aligned} \frac{dI}{dt} &= k_1 I\left(1 - \frac{I}{I_{max}}\right) - k_2 IE - \gamma IN \\ \frac{dE}{dt} &= k_3\left(1 - \zeta\frac{N}{\phi_E + N}\right)\frac{IE}{k_p + I} - k_4\frac{IE}{k_e + I} \\ \frac{dN}{dt} &= k_5\left(\frac{I}{\phi_N + I} - N\right) \end{aligned} \qquad [S6]$$

Here, we let the NK cell response, N, rise in proportion to the antigen load, I, in a saturable manner with the scaling constant ϕ_N and decay with the rate constant k_5. Further, we let the NK cells eliminate infected cells at the rate γ and suppress the CD8 T cell response by the maximal extent ζ. The remaining terms are similar to those in Eq. 1 in the main text.

Solving the equations for steady states and performing linear stability analysis yielded two stable and one unstable steady state (Fig. S3). The stable steady states represented persistence and clearance. These steady states were separated by the basin boundary, which was now a surface in 3D, on which the unstable saddle node was located. Representative trajectories beginning on either side of the basin boundary, with and without NK cells, are illustrated in Fig. S3.

Text S4: Mathematical model of the motif with the innate immune response. The following equations describe the behavior of the motif with the innate immune response (Fig. 4):

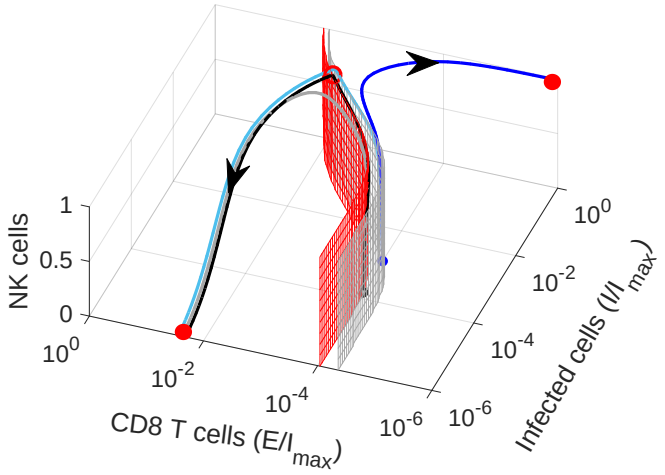

Fig. S3. Influence of NK cells. Trajectories corresponding to medium dose inocula with (black) and without (grey) NK cells and to high dose inocula with (light blue) and without (blue) NK cells are shown. The basin boundaries with (red) and without NK cells (grey) are also shown. Projections of the trajectories and basin boundaries are in Fig. 3.

$$\begin{aligned}\frac{dI}{dt} &= k_1\big(1-\epsilon\frac{X}{\phi_X+X}\big)I\big(1-\frac{I}{I_{max}}\big)-k_2IE\\ \frac{dE}{dt} &= k_3\frac{IE}{k_p+I}-k_4\frac{IE}{k_e+I}\\ \frac{dX}{dt} &= k_6\big(\frac{I}{\phi_I+I}-X\big)\end{aligned} \qquad [S7]$$

Here, X is a coarse-grained, normalized variable quantifying the innate immune response. X rises in proportion to the antigen load, I, in a saturable manner with the scaling constant ϕ_I and decays with the rate constant k_6. We assumed that X restricts the spread of infection with the maximal efficacy ϵ and the scaling constant ϕ_X. ϕ_I sets the scale of the antigen load that triggers the innate immune response. Large values of ϕ_I imply weak immune responses. The remaining terms are similar to those in Eq. 1 in the main text.

Solving the equations for steady states and performing linear stability analysis again yielded two stable and one unstable steady state (Fig. S4). The stable steady states represented persistence and clearance and were separated by a basin boundary, a surface in 3D, on which the unstable saddle node was located. Representative trajectories beginning on either side of the basin boundary, with strong and weak innate immune responses, are illustrated in Fig. S4. Projections of these trajectories and the basin boundary are shown in Fig. 4.

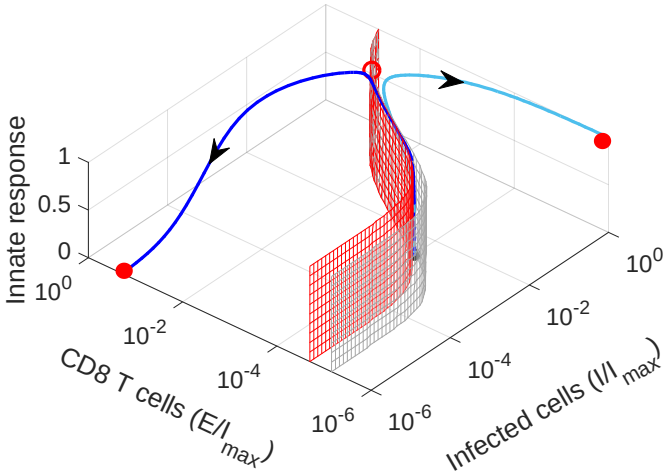

Fig. S4. Influence of the innate immune response. Trajectories corresponding to strong (dark blue) and weak (light blue) innate immune responses are shown. The basin boundaries with strong (grey) and weak (red) innate immune responses are also shown. Projections of the trajectories and basin boundaries are in Fig. 4.

Text S5: Model of HCV dynamics with innate immune response. We constructed a model of HCV dynamics that included our framework above of the innate immune response (Fig. 4A) in standard models of HCV kinetics (2, 3) (Fig. 5A). The model equations are as follows:

$$\begin{aligned}
\frac{dT}{dt} &= s + r_T T\big(1 - \frac{T+I}{T_{max}}\big) - d_T T - \beta V T + f_2 m I E \\
\frac{dI}{dt} &= \beta V T + r_I I\big(1 - \frac{T+I}{T_{max}}\big) - \delta I - m(f_1 + f_2) I E \\
\frac{dV}{dt} &= p\big(1 - \epsilon \frac{X}{\phi_X + X}\big) - cV \\
\frac{dX}{dt} &= k_6\big(\frac{I}{\phi_I + I} - X\big) \\
\frac{dE}{dt} &= \lambda \mathcal{H}(\tau_d) + k_3 \frac{IE}{k_p + I} - k_4 \frac{IE}{k_e + I} - \mu E
\end{aligned} \qquad [S8]$$

Here, T represents the population of target, uninfected hepatocytes; I, infected hepatocytes; V, virus; X, the innate immune response; and E, CD8 T cells. Target cells are produced at the rate s, proliferate at the per capita rate r_T, die at the per capita rate d_T, and are infected by virions at the rate βVT, to yield infected cells. The latter cells proliferate at the per capita rate r_I, and die at the per capita rate δ. Total cell proliferation is restricted by a logistic term with carrying capacity T_{max}. Virus is produced at the rate p per infected cell and cleared at the per capita rate c. These latter steps represent details of antigenic growth that we had subsumed into the proliferation of infected cells in our dynamical motif (Fig. 1A).

We let the innate immune response follow the form above (Eq. S7). The response suppresses viral production (2), which we assumed to occur with the maximal efficacy ϵ. For CD8 T cell dynamics, we followed earlier models of activation and exhaustion (1, 4) together with a delay in the induction of the response (5–7), characterized using τ_d (3). $\mathcal{H}$ represents the Heaviside function such that $\mathcal{H}(x) = 0$ if $x < 0$ and $\mathcal{H}(x) = 1$ if $x \geq 0$. CD8 T cells are thus produced at the rate λ after a delay of τ_d following the onset of infection and die at the per capita rate μ. Their effect on infected cells is both cytolytic and non-cytolytic (3). We represented the two effects using the terms f_1 and f_2, respectively. Thus, infected cells are destroyed at the rate mf_1IE and recover and become target cells at the rate mf_2IE.

References

1. Johnson PLF et al. (2011) Vaccination alters the balance between protective immunity, exhaustion, escape, and death in chronic infections. *J Virol* 85:5565–5570.
2. Neumann AU et al. (1998) Hepatitis C viral dynamics in vivo and the antiviral efficacy of interferon-α therapy. *Science* 282:103–107.
3. Dahari H et al. (2005) Mathematical modeling of primary hepatitis C infection: Noncytolytic clearance and early blockage of virion production. *Gastroenterology* 128:1056–1066.
4. Conway JM, Perelson AS (2015) Post-treatment control of HIV infection. *Proc Natl Acad Sci U S A* 6:5467–5472.
5. Major ME et al. (2004) Hepatitis C virus kinetics and host responses associated with disease and outcome of infection in chimpanzees. *Hepatology* 39:1709–1720.
6. Shin E et al. (2011) Delayed induction, not impaired recruitment, of specific CD8 + T cells causes the late onset of acute hepatitis C. *Gastroenterology* 141:686–695.
7. Thimme R et al. (2001) Determinants of viral clearance and persistence during acute hepatitis C virus infection. *J Exp Med* 194:1395–1406.
8. Bocharov GA (1998) Modelling the dynamics of LCMV infection in mice: Conventional and exhaustive CTL responses. *J Theor Biol* 192:283–308.
9. Keşmir C, De Boer RJ (2003) Clonal exhaustion as a result of immune deviation. *Bull Math Biol* 65:359–374.
10. Baral S, Roy R, Dixit NM (2018) Modeling how reversal of immune exhaustion elicits cure of chronic hepatitis C after the end of treatment with direct-acting antiviral agents. *Immunol Cell Biol* 96:969–980.

Table S1. Parameter estimates. The parameter values employed in our model calculations are listed along with ranges available in the literature. Where no estimates were available, we have assumed parameters values to ensure that the key qualitative features of the system are maintained.

Parameter	Meaning	Value	Range or value from literature	Source
		Figs. 1 & 2		
k_1	Infection spread rate	1.3/day	$3-4$/day	(8, 9)
I_{max}	Maximum number of infected cells	10^6 cells	10^6 cells	(1)
k_2	Killing rate of infected cells by CD8 T cells	5×10^{-5}/cells/day	$\sim10^{-6}-10^{-4}$ /cells/day	(8, 9)
k_3	Antigen driven CD8 T cell proliferation rate	1/day	~ 1/day	(1, 4, 10)
k_4	Antigen driven CD8 T cell suppression rate	3/day	$2-4$/day	(1, 4, 10)
k_p	Antigen driven proliferation threshold	10 cells	$10^{-1}-10^3$ cells	(1, 4)
k_e	Antigen driven suppression threshold	2×10^5 cells	$5-2.7\times10^4$ cells	(4, 10)
α	Rate of growth of cytokine pathology	10^{-8} /cells^2/day		
d_c	Rate of loss of cytokine pathology	1/day		
		Fig. 3		
k_1	Infection spread rate	1.5/day	$3-4$/day	(8, 9)
I_{max}	Maximum number of infected cells	10^6 cells	10^6 cells	(1)
k_2	Killing rate of infected cells by CD8 T cells	4×10^{-4}/cells/day	$10^{-6}-10^{-4}$	(8, 9)
k_3	Antigen driven CD8 T cell proliferation rate	1.55/day	~ 1/day	(1, 4, 10)
k_4	Antigen driven CD8 T cell suppression rate	3/day	$2-4$/day	(1, 4, 10)
k_p	Antigen driven proliferation threshold	1000 cells	$10^{-1}-10^3$ cells	(1, 4)
k_e	Antigen driven suppression threshold	1×10^5 cells	$5-2.7\times10^4$ cells	(4, 10)
k_5	NK cell activation rate	5/day		
	NK cell activation rate with NK cell depletion	0/day		
ϕ_N	NK cell activation threshold	100 cells		
ζ	Efficacy of NK cell suppression of CD8 T cell proliferation	0.3		
ϕ_E	NK cell efficacy threshold	0.5 cells		
γ	Rate of elimination of infected cells by NK cells	0.1 /cells/day		
α	Rate of growth of cytokine pathology	10^{-8} /cells^2/day		
d_c	Rate of loss of cytokine pathology	1/day		
		Fig. 4		
k_1	Infection spread rate	1.5/day	$3-4$/day	(8, 9)
I_{max}	Maximum number of infected cells	10^6 cells	10^6 cells	(1)
k_2	Killing rate of infected cells by CD8 T cells	4×10^{-5}/cells/day	$10^{-6}-10^{-4}$	(8, 9)
k_3	Antigen driven CD8 T cell proliferation rate	1.55/day	~ 1/day	(1, 4, 10)
k_4	Antigen driven CD8 T cell suppression rate	3/day	$2-4$/day	(1, 4, 10)
k_p	Antigen driven proliferation threshold	1000 cells	$10^{-1}-10^3$ cells	(1, 4)
k_e	Antigen driven suppression threshold	1×10^5 cells	$5-2.7\times10^4$ cells	(4, 10)
k_6	Innate immune response activation rate	10/day		
ϕ_I	Innate immune response activation threshold (strong response)	200 cells		
	Innate immune response activation threshold (weak response)	2000 cells		
ζ	Efficacy of innate immune response suppression of viral replication	0.95		
ϕ_X	Efficacy threshold for innate immune response	0.8 cells		
α	Rate of growth of cytokine pathology	10^{-8} /cells^2/day		
d_c	Rate of loss of cytokine pathology	1/day		

Table S2. Parameter values used for our calculations of HCV dynamics (Fig. 5).

Parameters	Meaning	Value	Source
s	Target cell production rate	$d_T T_{max}$	(3)
r_T	Target cell proliferation rate	0.53/day	(3)
T_{max}	Carrying capacity of liver	7×10^7 cells/mL	(3)
d_T	Target cell death rate	0.0034 /day	(3)
β	Infection rate constant	1×10^{-8} mL/cells/day	(3)
r_I	Infected cell proliferation rate	0.53/day	(3)
δ	Death rate of infected cells	$1.5 \times d_T$	(3)
m	Effector strength of CTL response	5.2 mL/cells/day	
f_1	Cytolytic fraction of CTL response	0.3	(3)
f_2	Non-cytolytic fraction of CTL response	0.7	(3)
p	Virus production rate	20 virions/cell/day	(3)
ϵ	Efficacy of innate immune response in blocking viral production	0.99	(3)
ϕ_X	Efficacy threshold for innate immune response	0.1 cells/mL	
k_6	Innate immune response activation rate	5/day	
ϕ_I	Innate immune response activation threshold (strong response)	10^4 cells/ml	
	Innate immune response activation threshold (weak response)	4×10^5 cells/mL	
λ	CD8 T cell recruitment rate	1 cells/mL/day	(4)
k_3	Antigen driven CD8 T cell proliferation rate	1/day	(4)
k_4	Antigen driven CD8 T cell suppression rate	2/day	(4)
k_p	Antigen driven CD8 T cell proliferation threshold	500 cells/mL	(4)
k_e	Antigen driven CD8 T cell suppression threshold	1000 cells/mL	
μ	Death rate of CD8 T cells	2/day	(4)